Structure and rheology of ferrofluids: simulation results and kinetic models

2006 J. Phys.: Condens. Matter 18 S2757

(http://iopscience.iop.org/0953-8984/18/38/S15)

INSTITUTE OF PHYSICS PUBLISHING JOURNAL OF PHYSICS: CONDENSED MATTER

J. Phys.: Condens. Matter **18** (2006) S2757–S2770 doi:10.1088/0953-8984/18/38/S15

Structure and rheology of ferrofluids: simulation results and kinetic models

Patrick Ilg[1,2], **Eric Coquelle**[1] **and Siegfried Hess**[1]

[1] Institut für Theoretische Physik, Technische Universität Berlin, Hardenbergstraße 36, D-10623 Berlin, Germany
[2] Polymer Physics, ETH Zürich, Department of Materials, CH-8093 Zürich, Switzerland

E-mail: ilg@physik.tu-berlin.de

Received 1 May 2006
Published 8 September 2006
Online at stacks.iop.org/JPhysCM/18/S2757

Abstract

Magnetoviscous and viscoelastic phenomena in ferrofluids are intimately related to their internal structures. The available kinetic models describing the rheological behaviour rely on strong assumptions and simplifications of these structures. Using equilibrium and nonequilibrium computer simulations, here we discuss the validity of the crucial assumption of rigid, chain-like aggregates underlying the chain model. The simulation results support the existence of chain-like aggregates in strongly interacting ferrofluids, at least for sufficiently strong magnetic fields. In addition, shear-induced degradation of the clusters is observed, which apparently is related to strong shear thinning behaviour. For weakly interacting ferrofluids, only slightly anisotropic spatial structures are observed. In this regime, the simulation results of the magnetoviscous effect are in good agreement with the predictions of a dynamical mean-field theory. Further, we explore some first steps towards a unified kinetic model that is applicable in both, the weakly and strongly interacting regimes.

1. Motivation

Recent experimental results on strongly interacting cobalt ferrofluids have revealed a huge magnetoviscous effect, strong shear thinning behaviour as well as shear-induced structural changes [1, 2]. Despite its strong assumptions, the so-called chain model [3, 4] appears to provide the best theoretical description of these phenomena in strongly interacting ferrofluids available at present [5, 6]. It has been shown recently, that a slightly modified version of the chain model is able to predict the equilibrium magnetization very accurately also for intermediate interaction strengths [7]. However, it has been argued that the assumption of rigid, rod-like aggregates underlying the chain model is an oversimplification and that the flexibility of the chains has a significant influence on the equilibrium properties [8–10]. As far as flow properties are concerned, the assumption of rigid, rod-like aggregates seems even more problematic. From polymer kinetic theory, for example, it is known that the degree of

chain flexibility has a major effect on dynamical properties [11]. The chain model was recently extended to strong flow regimes by introducing phenomenologically a maximum chain length in order to capture the effect of flow-induced breaking of chains [5].

In the following, we address some of the main assumptions made within the chain model by comparison with equilibrium (BD) and non-equilibrium Brownian dynamics (NEBD) simulations. For weak dipolar interactions, no chain-formation occurs and the chain model is inapplicable. In this regime, systematic cluster [12] and perturbation expansions [13] have been employed, which predict equilibrium properties very accurately [7, 14]. An extension of these approaches to describe rheological behaviour within a dynamical mean-field theory has been proposed in [15, 16]. Comparisons to simulation results show that the dynamical mean-field (DMF) model provides an accurate description in the weakly interacting regime. Apparently, the chain model and DMF model are applicable in different regimes. A unified model that is valid for all interaction strengths would be desirable.

The remainder of this paper is organized as follows. The model system, the interaction potential, as well as the time evolution equations are defined in section 2. Equilibrium properties of the model are discussed in section 3. Section 4 deals with structural and rheological properties of the model in shear flow. Thereby, the regime of weak interactions is considered in section 4.1, while strongly interacting ferrofluids are treated in section 4.2. Some first steps towards a unified kinetic model applicable in the weak and strongly interacting regime are explored in section 5, before some conclusions are offered in section 6.

2. Model formulation

The ferrofluid model studied here is identical or very similar to those studied in previous works [14, 17–26].

2.1. Interaction potential

The model system under study consists of N interacting spherical particles in a volume V with number density $\rho = N/V$. Let $\boldsymbol{r}_i$ and $\boldsymbol{m}_i$ denote the position and embedded magnetic point dipole of particle i, respectively. In the presence of a magnetic field $\boldsymbol{H}$, the magnetic dipole $\boldsymbol{m}_i$ contributes $U_H(i) = -\mu_0 \boldsymbol{m}_i \cdot \boldsymbol{H}$ to the total potential energy U of the system, which is given by $U = \sum_i U_H(i) + \sum_{i<j} \Phi(ij)$. The interaction potential between two particles is

$$\Phi(12) = \Phi_s(r_{12}) + \frac{\mu_0 m_1 m_2}{4\pi r_{12}^3}\left[\boldsymbol{u}_1 \cdot \boldsymbol{u}_2 - 3(\boldsymbol{u}_1 \cdot \hat{\boldsymbol{r}}_{12})(\boldsymbol{u}_2 \cdot \hat{\boldsymbol{r}}_{12})\right], \tag{1}$$

where 1 (2) denotes the spatial and orientational coordinate of particle 1 (2) and $r_{12} = |\boldsymbol{r}_{12}|$ the distance between particle 1 and 2 with $\boldsymbol{r}_{12} = \boldsymbol{r}_1 - \boldsymbol{r}_2$. The strength and orientation of the magnetic moment of particle i is denoted by m_i and $\boldsymbol{u}_i$, respectively, and $\hat{\boldsymbol{r}}_{12} = \boldsymbol{r}_{12}/r_{12}$. Here we consider a monodisperse system with $m_i = m$. The magnetic field and dipolar interactions introduce two energy scales into the system. Their respective strengths relative to the thermal energy is measured by the Langevin parameter α and dipolar interaction parameter λ,

$$\alpha = \frac{\mu_0 m H}{k_B T}, \qquad \lambda = \frac{\mu_0 m^2}{4\pi k_B T d_m^3}, \tag{2}$$

where $H = |\boldsymbol{H}|$ and d_m denotes the magnetic diameter of the particles. In order to prevent permanent agglomeration, the magnetic particles are usually covered with a polymeric shell [27]. The resulting steric interactions between the magnetic particles is modelled by the potential $\Phi_s(r)$. Specifically, a repulsive Lennard-Jones potential or an entropic repulsion proposed by Rosensweig [27] is employed. In the former case, $\Phi_s(r) = 4\varepsilon[C(r) - C(r_c)]$,

$C(r) = (d_\mathrm{m}/r)^{12} - (d_\mathrm{m}/r)^6$ for $r \leqslant r_\mathrm{c}$ and $\Phi_\mathrm{s}(r) = 0$ else, with $r_\mathrm{c} = 2^{1/6} d_\mathrm{m}$. This potential was chosen, for example, in [14, 22–25]. The interpretation of the Lennard-Jones energy parameter ε in ferrofluids is, however, not obvious. Therefore, Rosensweig's potential is sometimes preferred [17–21]. By considering the entropic repulsion of two rod-like polymers attached to solid walls, Rosensweig estimated the interaction potential of two polymer-coated spheres as [27]

$$\Phi_\mathrm{s}(r) = \begin{cases} \dfrac{N_\mathrm{p} k_\mathrm{B} T}{2\delta} \left\{ \tilde{d}_\mathrm{h} + r[\ln(\tilde{d}_\mathrm{h}/r) - 1] \right\} & \text{for } d_\mathrm{m} \leqslant r \leqslant \tilde{d}_\mathrm{h} \\ 0 & \text{else.} \end{cases} \tag{3}$$

The number of polymer molecules on the surface and their effective lengths are denoted by N_p and δ, respectively. The quantity $\tilde{d}_\mathrm{h} = d_\mathrm{m} + 2\delta$ gives the range of the repulsive interaction. Typical values are $N_\mathrm{p} \approx 100$–300 and $\delta \approx 2$ nm [27]. We assume the stabilizing shell to be thick enough, such that van der Waals attraction can be neglected.

2.2. Model dynamics

As was done in previous studies, we assume that the particles are magnetically hard, i.e. they are large enough such that the magnetic moment remains frozen within the particle [27]. The magnetic particles experience friction forces and torques due to the solvent, leading to an overdamped motion [11], which is often called Brownian dynamics (BD). In the presence of a macroscopic flow field $\boldsymbol{V}(\boldsymbol{r})$ with vorticity $\boldsymbol{\Omega}(\boldsymbol{r}) = \frac{1}{2}\nabla_r \times \boldsymbol{V}(\boldsymbol{r})$, the corresponding non-equilibrium Brownian dynamics (NEBD) reads [21, 28]

$$\mathrm{d}\boldsymbol{r}_i = \left[\boldsymbol{V}(\boldsymbol{r}_i) + \xi_\mathrm{t}^{-1} \boldsymbol{F}_i\right] \mathrm{d}t + \sqrt{2D_\mathrm{t}}\, \mathrm{d}\boldsymbol{W}_{\mathrm{t},i} \tag{4}$$

$$\mathrm{d}\boldsymbol{u}_i = (\boldsymbol{1} - \boldsymbol{u}_i \boldsymbol{u}_i) \cdot [(\boldsymbol{\Omega} + \xi_\mathrm{r}^{-1} \boldsymbol{N}_i) \times \boldsymbol{u}_i \, \mathrm{d}t + \sqrt{2D_\mathrm{r}}\, \mathrm{d}\boldsymbol{W}_{\mathrm{r},i}] - D_\mathrm{r} \boldsymbol{u}_i \, \mathrm{d}t. \tag{5}$$

The potential forces and torques are given by $\boldsymbol{F}_i = -\nabla_{r_i} U$ and $\boldsymbol{N}_i = -\boldsymbol{\mathcal{L}}_i U$, respectively, with the rotational operator $\boldsymbol{\mathcal{L}}_i = \boldsymbol{u}_i \times \partial/\partial \boldsymbol{u}_i$. $\boldsymbol{W}_{a,i}$, $a = \{\mathrm{t}, \mathrm{r}\}$ denote three-dimensional, independent Wiener processes. We adopt the Itô interpretation of the stochastic differential equation (5) such that the norm of the unit vector is strictly conserved, $\mathrm{d}(\boldsymbol{u}_i^2) = 0$ due to Itô's formula [28].

The single-particle translational and rotational diffusion coefficients are related to the corresponding friction coefficients by $D_a = k_\mathrm{B} T/\xi_a$. For hard spheres of diameter d_h, the translational and rotational friction coefficients appearing in equations (4), (5) are given by $\xi_\mathrm{t} = 3\pi\eta_\mathrm{s} d_\mathrm{h}$ and $\xi_\mathrm{r} = \pi\eta_\mathrm{s} d_\mathrm{h}^3$, respectively, where η_s denotes the viscosity of the solvent. For smooth repulsive interactions $\Phi_\mathrm{s}(r)$, a hydrodynamic diameter d_h is defined with the help of the equivalent hard sphere diameter $d_\mathrm{h} = \int_0^\infty \mathrm{d}r\, (1 - \exp[-\beta\Phi_\mathrm{s}(r)])$, $\beta = (k_\mathrm{B} T)^{-1}$, as proposed by Barker and Henderson [29]. Since Φ_s vanishes for $r \geqslant \tilde{d}_\mathrm{h}$, the equivalent hard sphere diameter is smaller than the range of Rosensweig's repulsive interaction potential $d_\mathrm{h} \leqslant \tilde{d}_\mathrm{h}$. The alternative definition $\Phi_\mathrm{s}(d_\mathrm{h}) \equiv k_\mathrm{B} T$ leads to very similar values. It should be noted that, due to the steric repulsion, the minimal distance between particles is given by d_h instead of d_m. Therefore, the dipole–dipole energy of two dipoles aligned head-to-tail at contact is $-2\lambda^* k_\mathrm{B} T$, with $\lambda^* = (d_\mathrm{m}/d_\mathrm{h})^3 \lambda$. For this reason, it has been emphasized [30] that the physically relevant quantity is λ^* rather than λ. For a typical ferrofluid, $d_\mathrm{m} \approx 10$ nm, $d_\mathrm{h} \approx 12$–14 nm, and λ^* is smaller than λ by a factor of 2–3.

Equations (4), (5) describe the time evolution of the interacting N-particle system subject to a given flow field. Numerical solutions of the model by NEBD simulations are presented in the following sections together with different approximations to the full model systems. In

particular, we will be interested in the case of planar Couette flow $\boldsymbol{V}(\boldsymbol{r}) = \dot{\gamma} y \boldsymbol{e}^x$ with shear rate $\dot{\gamma}$.

It should be mentioned that equations (4), (5) apply in the so-called free-draining limit where hydrodynamic interactions between colloidal particles can be neglected. These interactions arise due to flow disturbances of the solvent which are created by moving colloidal particles and felt by other particles [31]. Brownian dynamics simulations of ferrofluids including hydrodynamic interactions for neighbouring particles have been carried out in [17, 18]. Unfortunately, no estimation on the importance of hydrodynamic interactions was made therein. Preliminary results on diffusion coefficients [32] seem to indicate only mild influence of hydrodynamic interactions on the dynamics. Work in this direction is currently in progress.

2.3. Definition of macroscopic quantities

The macroscopic magnetization of the system is given by the ensemble average of the individual magnetic moments, $\boldsymbol{M} = M_{\mathrm{sat}} \langle \boldsymbol{u} \rangle$, where $M_{\mathrm{sat}} = \rho m$ is the saturation magnetization and $\langle \boldsymbol{u} \rangle = N^{-1} \sum_{j=1}^{N} \boldsymbol{u}_j$ denotes the average orientation of the magnetic dipoles.

The definition of the pressure tensor in magnetic fluids has been the subject of a number of studies [2]. The orientational motion leads to an antisymmetric contribution to the viscous pressure tensor $\boldsymbol{p}^{\mathrm{a}}$ if the average angular velocity of the particles $\langle \boldsymbol{\omega} \rangle$ does not match the local vorticity of the flow, $\boldsymbol{p}^{\mathrm{a}} = 3\eta_{\mathrm{s}}\phi\, \boldsymbol{\epsilon} \cdot (\langle \boldsymbol{\omega} \rangle - \boldsymbol{\Omega})$ [11]. The total antisymmetric tensor of rank three (Levi-Civita) is denoted by $\boldsymbol{\epsilon}$. Inserting $\boldsymbol{\omega}_i$ from equation (5) and averaging over the particles, one obtains the familiar expression $\boldsymbol{p}^{\mathrm{a}} = \mu_0 \boldsymbol{M} \times \boldsymbol{H}$. Summing the viscous and Maxwell's magnetic pressure tensor, $\boldsymbol{P}_{\mathrm{M}} = -\boldsymbol{B}\boldsymbol{H} + p_{\mathrm{M}} \mathbb{1}$ with $\boldsymbol{B} = \mu_0(\boldsymbol{H} + \boldsymbol{M})$ [33], the total pressure tensor is found to be symmetric, expressing the conservation of total angular momentum. Using the standard virial expression [34] for the symmetric traceless part, the total viscous pressure tensor is given by

$$\boldsymbol{P} = p\mathbb{1} - 2\eta_{\mathrm{s}}\boldsymbol{\Gamma} + \frac{1}{2V} \sum_{j<k}^{N} \overline{\boldsymbol{r}_{jk} \boldsymbol{F}_{jk}} + \frac{\mu_0}{2}(\boldsymbol{M}\boldsymbol{H} - \boldsymbol{H}\boldsymbol{M}), \tag{6}$$

where $\boldsymbol{\Gamma} \equiv \frac{1}{2}[\nabla_{\boldsymbol{r}} \boldsymbol{v} + (\nabla_{\boldsymbol{r}} \boldsymbol{v})^{\mathrm{T}}]$ is the symmetric velocity gradient, $\boldsymbol{F}_{12} = -\nabla_{\boldsymbol{r}_1} \Phi(12)$ and $\overline{\ldots}$ denotes the symmetric traceless part.

In a planar shear flow, $\boldsymbol{V}(\boldsymbol{r}) = \dot{\gamma} y \boldsymbol{e}^x$, the shear viscosity is defined by $\eta = -P_{xy}/\dot{\gamma}$. Note that no contribution of the Maxwell pressure tensor to the shear stress arises because of the boundary conditions for the magnetic fields $\boldsymbol{H}$ and $\boldsymbol{B}$ (see e.g. chapter 8.12. of [27]). Similarly to the Miesowicz viscosities of liquid crystals [11, 26, 35], different viscosity coefficients η_i can be defined if the magnetic field is oriented in flow ($i = 1$), in gradient ($i = 2$), or in the vorticity direction ($i = 3$). In addition, a fourth viscosity coefficient is needed to fully characterize the viscous behaviour. This coefficient can be chosen as η_4, the viscosity that is measured if the magnetic field is oriented along the bisector of the flow and gradient direction.

2.4. NEBD simulations

The coupled dynamical equations (4) and (5) are solved numerically for a system of $N = 10\,976$ particles. A second-order predictor–corrector scheme was used for the translational motion (4), while a first-order scheme was employed for the rotational dynamics which conserves exactly the norm of the unit vectors $\boldsymbol{u}_i$ [28]. The long-range parts of the dipolar interactions were treated by the reaction field method [24]. The cut-off radius was chosen as

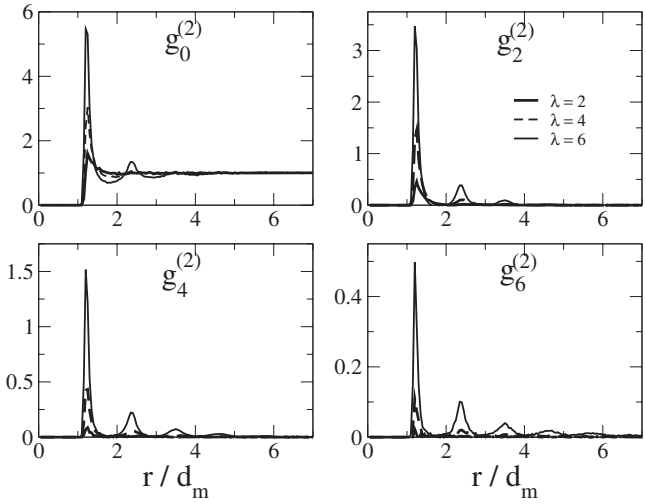

Figure 1. Equilibrium pair correlation functions $g_j^{(2)}$ defined in the text as a function of distance for different dipolar interaction strengths. All data were obtained in the presence of a magnetic field with strength $\alpha = 10$. Further parameters are $\phi = 0.05$, $N_\mathrm{p} = 314$ and $\tilde{d}_\mathrm{h}/d_\mathrm{m} = 1.2$ for the steric potential (3).

$r_\mathrm{cut} = 5\,d_\mathrm{m}$. Some tests with a larger value of $8\,d_\mathrm{m}$ gave very similar results. Lees–Edwards periodic boundary conditions were employed to deal with shear flows in finite systems. Starting from arbitrary initial conditions, the system was evolved until a stationary state was reached. With a typical time step of $\Delta t = 3 \times 10^{-4}\tau_\mathrm{B}$, the equations were numerically integrated for 3×10^5 steps. We verified that the system had reached a stationary state after this time. Structural and rheological data were extracted from time averages for another integration period of 4×10^5 time steps.

3. Equilibrium structure

Like other complex fluids, ferrofluids show interesting equilibrium properties due to their internal structure. It is therefore important to understand the equilibrium properties before studying their dynamical behaviour [11, 36]. Determining the equilibrium structure of dipolar fluids is a long-standing issue in statistical physics [37–39]. For weak dipolar interactions, perturbation theories around an ideal reference state apply [13, 40], leading to weakly anisotropic structures. For strong dipolar interactions, on the other hand, the formation of chain-like structures is expected [3, 4]. The dynamical and rheological behaviour in these regimes will be considered in section 4.

For anisotropic liquids with uniaxial symmetry around the direction $\hat{\boldsymbol{H}} = \boldsymbol{H}/H$, the pair correlation function $g^{(2)}$ can be expanded as $g^{(2)}(\boldsymbol{r}) = \sum_{j=0}^{\infty} c_j g_j^{(2)}(r) P_j(\hat{\boldsymbol{r}} \cdot \hat{\boldsymbol{H}})$ with $c_j = [4\pi(2j+1)]^{-1}$ and $g_j^{(2)}(r) = \int \mathrm{d}^2\hat{r}\, P_j(\hat{\boldsymbol{r}} \cdot \hat{\boldsymbol{H}}) g(\boldsymbol{r})$ [36, 41, 42]. For symmetry reasons, only even terms appear in this sum. While for isotropic liquids only $g_0^{(2)}$ is non-zero, the functions $g_j^{(2)}$ with $j \geqslant 2$ quantify the anisotropy of the structure. Figure 1 shows BD simulation results of $g_j^{(2)}$ for the model system described in section 2. The entropic repulsion (3) was chosen with $N_\mathrm{p} = 314$ and $\tilde{d}_\mathrm{h}/d_\mathrm{m} = 1.2$, leading to an equivalent hard sphere diameter of $d_\mathrm{h}/d_\mathrm{m} \approx 1.17$. Different dipolar interaction strengths $\lambda = 2$, 4, and 6 have been chosen, corresponding to $\lambda^* \approx 1.25$, 2.5, and 3.75, respectively. The magnetic field

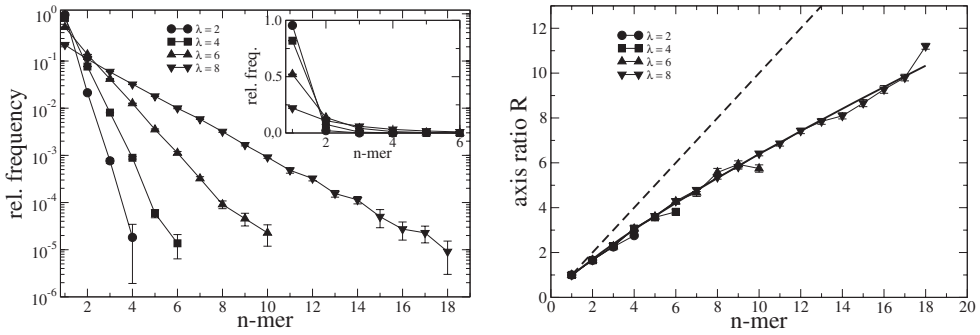

Figure 2. *Left*: equilibrium chain size distribution g_n on a semi-logarithmic scale in the presence of a magnetic field with $\alpha = 10$ for different dipolar interaction strengths λ. The same parameters as in figure1 have been chosen. The inset shows the same data but on a linear scale. *Right*: the axis ratio R of the clusters defined in the text as a function of the number n of particles in the cluster. The same conditions as in the left panel are chosen. Solid and dashed line correspond to $R = n^{\nu}$ with $\nu = 0.82$ and 1, respectively.

$\alpha = 10$ and the volume fraction $\phi = 0.05$ were held constant with $\phi_h \approx 0.08$. For weak dipolar interactions, the structures are almost isotropic and $g_0^{(2)}$ resembles the pair correlation function of a dilute gas. For strong dipolar interactions, however, figure 1 clearly shows the formation of anisotropic spatial structures with almost equally spaced maxima.

For sufficiently strong dipolar interactions, the formation of anisotropic, chain-like aggregates of magnetic particles has been observed in many simulations [37]. In thin films of iron ferrofluids, chain structures have been observed by cryo-TEM (transmission electron microscopy) imaging methods [43, 44]. Small-angle neutron scattering experiments suggest the existence of chain-like structures also in bulk ferrofluids under certain conditions [45].

Different methods have been used in order to calculate the average chain size $\langle n \rangle$ and the chain size distribution g_n. Here, we focus on the chain model, since this model has been extended successfully to also describe dynamical and rheological properties [3, 4]. The equilibrium chain size distribution g_n has been worked out in [3, 4], assuming rigid, rod-like aggregates with only nearest-neighbour interactions, also neglecting inter-chain interactions. The latter have been included recently within a mean-field approach [46]. For strong magnetic fields, the chain model predicts

$$g_n \propto \mathrm{e}^{-n/\langle n \rangle}, \qquad \langle n \rangle \propto \sqrt{\phi_h}\, \mathrm{e}^{\lambda^*}, \qquad \alpha \gg 1. \tag{7}$$

Analogous expressions have been derived for micellar solutions in [47].

Figure 2 shows g_n obtained from BD simulations of the model system described in section 2. The same parameters as in figure 1 have been chosen. Following [14], clusters are defined by an energy criterion: two particles are considered to be in the same cluster if their dipolar interaction energy is less than $E_{dd}/k_B T = -1.5\lambda^*$. Although the precise value of E_{dd} influences the calculated cluster sizes, similar results are obtained between $E_{dd}/k_B T = -1.7$ and -1.3. Remember that the minimal dipolar interaction energy at contact d_h is $E_{dd}/k_B T \approx -2\lambda^*$. From figure 2 we observe that significant chain formation occurs for $\lambda^* \gtrsim 3$, in agreement with results obtained in [14]. In addition, the chain size distributions g_n are found to decrease exponentially with n, in agreement with the prediction of the chain-formation model, equation (7).

In order to address the shape of the clusters, we define an effective axis ratio $R = \ell_\parallel / \ell_\perp$ of an n-cluster by its length in the field direction $\ell_\parallel = d_m + \sum_{i=1}^{n-1} |(\boldsymbol{r}_{i+1} - \boldsymbol{r}_i) \cdot \hat{\boldsymbol{H}}|$

and its extension in the perpendicular direction, $\ell_\perp = d_\mathrm{m} + \langle(\Delta r_\perp)^2\rangle^{1/2}$, with $(\Delta r_\perp)^2 = \sum_{i=1}^{n-1} |(\boldsymbol{r}_{i+1} - \boldsymbol{r}_i) \cdot (\mathbf{1} - \hat{\boldsymbol{H}}\hat{\boldsymbol{H}})|^2$. The dashed line in the right panel of figure 2 corresponds to a rod-like aggregate with $R = n$. The axis ratio of the clusters observed in the simulations increases as $R = n^\nu$ with $\nu \approx 0.82 \pm 0.05$. With the exponent ν intermediate between rigid rod-like ($\nu = 1$) and random coil behaviour ($\nu \approx 0.6$ with excluded volume interactions [11]), the aggregates can at least be considered as chain-like due to their moderate size. It is interesting to note that the increase $R = n^{0.8}$ seems to be roughly the same for all cluster sizes $n \leqslant 18$ observed and investigated here.

4. Non-equilibrium structure and rheology of ferrofluids

The kinetic model of isolated magnetic dipoles proposed in [48–50] has been used extensively over the last few years in order to explain magnetoviscous effects in ferrofluids (see, for example, [51] and Shliomis in [2]). The idealization of non-interacting particles, however, is a serious limitation of the theory, such that the model is applicable only for dilute ferrofluids with weak dipolar interactions. Improved theories that incorporate dipolar interactions are discussed in sections 4.1 and 4.2, together with some comparisons to simulation results.

4.1. Rheology of weakly interacting ferrofluids

In the weakly interacting regime, systematic cluster expansion and perturbation theory provide accurate descriptions for the equilibrium magnetization of ferrofluids [14]. Building upon these results, a dynamical mean-field theory has been proposed in [15] that incorporates weak dipolar interactions and flow-induced structural changes. With the help of the effective field approximation, explicit expressions for the viscosity coefficients η_i are derived in [15],

$$\eta_i = \eta_0 + \frac{3}{2}\eta_\mathrm{s}\phi_\mathrm{h}\frac{3S_1^2}{2+S_2}\left[(1-\delta_{i,3}) + \tilde{c}_i\kappa\chi_\mathrm{L}\frac{2+S_2}{3}\right], \tag{8}$$

where $i = 1$, 2, and 3 correspond to orientations of the magnetic field in flow, gradient, and vorticity direction, respectively. The coefficients $\tilde{c}_i$ are defined in [15] and depend on the detailed shape of the steric potential. The parameter κ is given by $\kappa = 72\tau_g/35\tau_\mathrm{B}$, where τ_g denotes a translational relaxation time. For weak flows, the orientational order parameters S_j can be approximated by their equilibrium values $S_j = L_j(\alpha_\mathrm{e})$, where $L_2(x) = 1 - 3L_1(x)/x$ and $L_1(x) = \coth(x) - x^{-1}$, the Langevin function. Then, the reduced effective field α_e can be taken from the modified mean-field approximation [52], $\alpha_\mathrm{e} = \alpha + \chi_\mathrm{L}L_1(\alpha)$. In the absence of dipolar interactions, equation (8) reduces to the familiar expression of the non-interacting model, $\eta_i = \eta_0 + \frac{3}{2}\eta_\mathrm{s}\phi_\mathrm{h}\alpha L_1^2(\alpha)/[\alpha - L_1(\alpha)]$.

Figure 3 shows the relative viscosity increase $\Delta\eta/\eta(0) = [\eta_2(\alpha) - \eta(0)]/\eta(0)$ as a function of the Langevin parameter α, where the magnetic field was oriented in gradient direction of the flow. NEBD simulations of the model system described in section 2 have been performed with $\phi = 0.07$ and $\lambda = 1.3$. The entropic repulsion (3) has been chosen with $N_\mathrm{p} = 314$ and $\tilde{d}_\mathrm{h}/d_\mathrm{m} = 1.4$, leading to an equivalent hard sphere diameter of $d_\mathrm{h}/d_\mathrm{m} \approx 1.35$, such that $\phi_\mathrm{h} \approx 0.17$ and $\lambda^* \approx 0.53$. A very weak dependence of $\Delta\eta/\eta(0)$ on the shear rate is observed. The simulation results are in good agreement with the predictions of the DMF model with $\tau_g/\tau_\mathrm{B} = 1$, whereas the model of non-interacting dipoles underpredicts the magnetoviscous effect. A detailed comparison with simulation results of the model system adopting the truncated Lennard-Jones potential showed the validity of the DMF model for weak dipolar interaction strengths $\lambda^* \lesssim 0.5$ [24, 25].

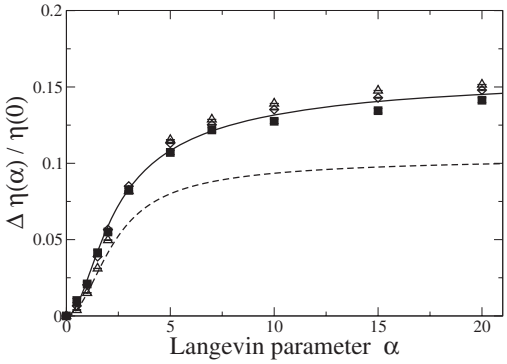

Figure 3. Relative viscosity increase as a function of the Langevin parameter α. Symbols are NEBD simulation results for different shear rates, the solid line is the prediction of the DMF model, the dashed line corresponds to the non-interacting model. Parameters are chosen as $\phi = 0.07$, $\lambda = 1.3$, $N_\mathrm{p} = 314$, $\tilde{d}_\mathrm{h}/d_\mathrm{m} = 1.4$, resulting in $\phi_\mathrm{h} \approx 0.17$ and $\lambda^* \approx 0.53$.

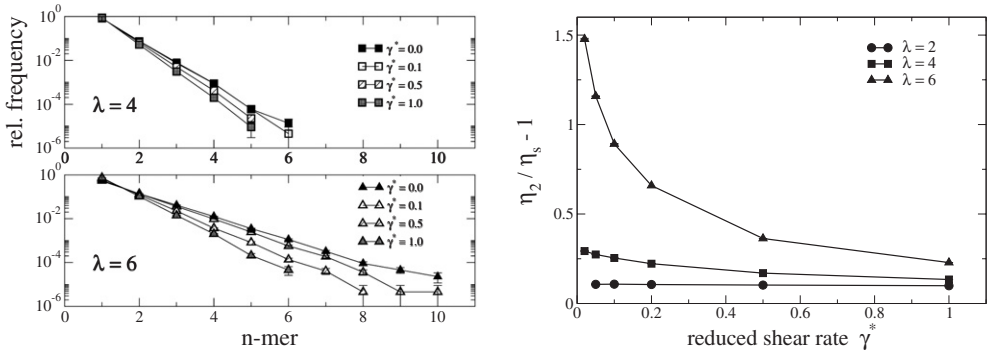

Figure 4. *Left*: non-equilibrium chain size distribution g_n on a semi-logarithmic scale for different shear rates $\dot{\gamma}^*$. The same parameters as in figure 1 have been chosen. *Right*: shear viscosity η/η_s as a function of shear rate.

4.2. Rheology of strongly interacting ferrofluids

The equilibrium, chain-like structures present in strongly interacting ferrofluids have a strong influence on the dynamical behaviour. For weak velocity gradients, the chain model assumes that the equilibrium chain size distribution g_n is not affected by the flow [3, 4]. In order to account for flow-induced structural changes that occur, for example, in strong shear flows [1], rupture of chains was introduced phenomenologically into the theory by imposing a maximum possible chain length n_c at a given shear rate [5]. The magnitude $n_\mathrm{c} \approx \frac{1}{3}\sqrt{\lambda^*/\dot{\gamma}^*}$, $\dot{\gamma}^* = \dot{\gamma}/2D_\mathrm{r}$, was estimated from the balance of dipolar and viscous forces [53].

Figure 4, left panel, shows the cluster size distribution in the presence of shear flow for various shear rates $\dot{\gamma}$. Here and below, the magnetic field is oriented in the gradient direction of the flow, if not stated otherwise. The other parameters have been chosen as in figure 1. The non-equilibrium cluster size distributions are still well described by an exponential form, however with a smaller average cluster size. The gradual decrease in large clusters with increasing shear rate is qualitatively consistent with the idea of shear-induced rupture of chains proposed in [5].

The right panel of figure 4 shows the shear viscosity η_2 normalized by η_s as a function of shear rate for the same conditions as used in the left panel. For the lowest dipolar interaction

strength $\lambda = 2$, hardly any chain formation is observed at all; see figure 2. Therefore, no dependence of η_2 on the shear rate is found. Increasing dipolar interaction strengths lead to an increase in shear viscosity. This increase is due to a larger contribution of the interparticle forces to the symmetric part of the viscous pressure, see equation (6), as well as due to an increase in the non-equilibrium magnetization. The shear-induced degradation of clusters observed in the left panel of figure 2 is reflected by a pronounced shear-thinning behaviour.

5. Towards a unified kinetic model

In sections 4.1 and 4.2, two different kinetic models of ferrofluid dynamics have been discussed. While the DMF model presented in section 4.1 is applicable for weak interactions, the chain model of section 4.2 deals with the strongly interacting regime. A unified model that is applicable for arbitrary interaction strengths would be highly desirable, but unfortunately does not exist at present.

Here, we explore some first, simple-minded steps in this direction. We start with the observation that the kinetic equation and the expression for the pressure tensor within the DMF model resemble the corresponding formulae for the chain model. Since both are simplified mean-field models, we might generously ignore the differences and *postulate* that the chain model applies also to the weakly interacting regime. In the non-interacting (NI) case, this is true since the chain model reduces to the NI model for spherical particles. For weak interactions, the shape parameter deduced from the DMF model is $B \approx -\frac{2}{7}\chi_{\mathrm{L}}$ [15]. A negative value of the shape parameter corresponds to oblate particles. No chain-like structures exist in this regime. However, the head-to-tail attraction and side-by-side repulsion of parallel magnetic moments by dipolar interactions can, in a mean-field sense, approximately be described by effective oblate particles. For strong dipolar interactions, the chain model in its original form applies. While strong dipolar interactions can lead to broad size distributions of chain-like clusters, we expect no such effects in the weakly interacting regime.

This very simple approach to a unified model of ferrofluid dynamics might serve as a useful starting point in guiding the way towards more sophisticated models. As a first test of this hypothesis, the translational self-diffusion in ferrofluids is studied within the chain model.

5.1. Translational diffusion

Anisotropic, field-dependent diffusion in ferrofluids has been observed in experiments, both for gradient diffusion [54–56] and self-diffusion [57]. The field dependence of the gradient diffusion coefficients have been studied theoretically in [58, 59]. A hydrodynamic theory of self-diffusion in ferrofluids is presented in [60, 61]. However, these studies were performed in the absence of a magnetic field.

In [62], one of the present authors proposes an approach to self-diffusion in ferrofluids within the chain model. In order to study translational diffusion, one needs to re-introduce translational motion into the chain model. The time-evolution of the spatial and orientational one-particle probability distribution function $\rho^{(1)}(\boldsymbol{r}, \boldsymbol{u}; t)$ can be written as $\partial_t \rho^{(1)} = (\hat{\mathrm{L}}_{\mathrm{r}}^{B} + \hat{\mathrm{L}}_{\mathrm{t}}^{B})\rho^{(1)}$, where $\hat{\mathrm{L}}_{\mathrm{r}}^{B}$ corresponds to the Fokker–Planck operator of the original chain model [3, 4]. For rigid ellipsoids, the translational part reads [11, 63, 64]

$$\hat{\mathrm{L}}_{\mathrm{trans}}^{B} \bullet = \nabla_r \cdot [D_{\parallel}^{0} \boldsymbol{u}\boldsymbol{u} + D_{\perp}^{0}(\mathbf{1} - \boldsymbol{u}\boldsymbol{u})] \cdot \{\beta[\nabla_r U] \bullet + \nabla_r \bullet\}, \tag{9}$$

where $D_{\parallel}^{0}$, $D_{\perp}^{0}$ are the parallel and perpendicular diffusion coefficients of the isolated chain-like aggregate, respectively. For spherical particles, one has $D_{\parallel}^{0} = D_{\perp}^{0}$. In equation (9), U is the mean-field interaction potential $U/k_{\mathrm{B}}T = -\alpha_{\mathrm{e}} \boldsymbol{u} \cdot \hat{\boldsymbol{H}}$, with the dimensionless

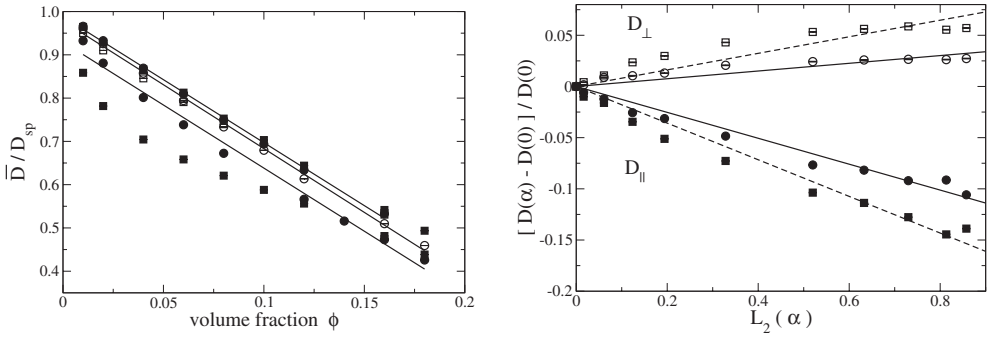

Figure 5. *Left*: average diffusion coefficient as a function of volume fraction. Circles and squares correspond to $\alpha = 0$ and 20, respectively, while solid and open symbols denote the results for $\lambda = 1$ and 4. *Right*: parallel and perpendicular diffusion coefficients are plotted versus the second Langevin function L_2 for $\lambda = 2$. Circles and squares correspond to $\phi = 0.02$ and 0.05, respectively. Adapted from [21].

effective field α_e. In view of the success of the modified mean-field approximation, we might choose $\alpha_e = \alpha + \chi_L L_1(\alpha)$. Due to the coupling of translational and orientational motion, anisotropic self-diffusion is found within this model. Explicit expressions for the parallel and perpendicular self-diffusion coefficients in terms of orientational order parameters are worked out in [62]. Results for both nematic liquid crystals and magnetic fluids are presented therein. For ferrofluids, the self-diffusion coefficients parallel and perpendicular to the magnetic field found in [62] read

$$D_\perp = \overline{D} - \tfrac{1}{3}(D_\parallel^0 - D_\perp^0) L_2(\alpha_e) c(\alpha_e)$$
$$D_\parallel = \overline{D} + \tfrac{2}{3}(D_\parallel^0 - D_\perp^0) L_2(\alpha_e) c(\alpha_e). \tag{10}$$

In equations (10), we have defined $c(\alpha_e) = 1 - \rho(\partial\alpha_e/\partial\rho) L_1(\alpha_e)$ and $L_2(x) = 1 - 3L_1(x)/x$. The average diffusion coefficient $\overline{D} \equiv (D_\parallel + 2D_\perp)/3$ is $\overline{D} = D^0 c(\alpha_e)$, where $D^0 = (D_\parallel^0 + 2D_\perp^0)/3$. In the dilute, weakly interacting regime, $\alpha_e \approx \alpha$. Using Maxwell's equation $\nabla \cdot (\boldsymbol{H} + \boldsymbol{M}) = \mathbf{0}$, we find $c(\alpha) = 1 + 3\chi_L L_1(\alpha)/[1 + 3\chi_L L_1'(\alpha)]$.

These predictions are tested for the ferrofluid model of section 2 by comparison to numerical simulations of the unapproximated model. Diffusion coefficients have been obtained numerically from the anisotropic, mean-square displacements of the particles in the course of the simulations. The average self-diffusion coefficient is found to decrease with increasing concentration (see left part of figure 5) and dipolar interaction strength, but to be independent of the magnetic field strength. These results are in agreement with the predictions of a simplified mean-field model [62]. In the presence of a magnetic field, the parallel and perpendicular diffusion coefficients are found to scale as $D_{\parallel,\perp} \propto L_2(\alpha)$, in agreement with the mean-field predictions (see right part of figure 5). Interestingly, we find $D_\parallel < D_\perp$ for moderate concentrations and dipolar interaction strengths, which corresponds to effective oblate particles. Note, however, that permanent, chain-like aggregates exist only for stronger dipolar interactions, where one expects a cross-over to $D_\parallel > D_\perp$. Further studies on diffusion properties in the strongly interacting regime would therefore be very interesting.

5.2. Consistency of the model?

The results on self-diffusion presented in the previous section are in agreement with the interpretation of effective oblate particles, which was suggested by the DMF model in the

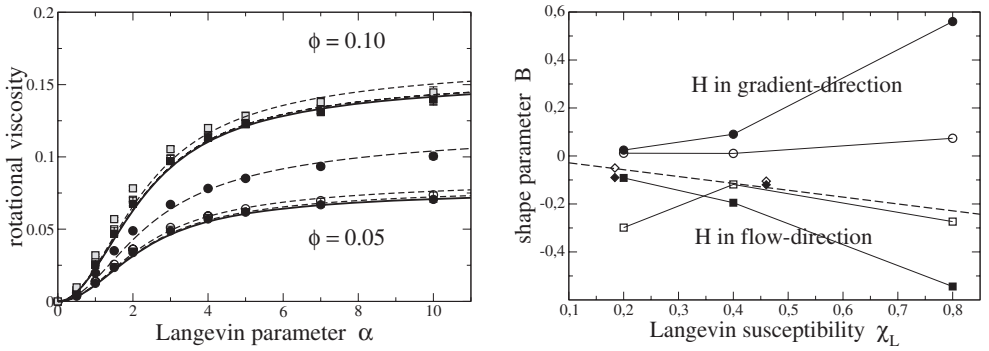

Figure 6. *Left*: rotational viscosity as a function of the Langevin parameter α. Squares and diamonds correspond to $\lambda = 0.25$ and 0.5, respectively. *Right*: shape parameter B as a function of the Langevin susceptibility, χ_L. Squares and circles indicate the magnetic field oriented in flow and in gradient direction, respectively. Filled and open symbols correspond to $\phi = 0.05$ and $\phi = 0.1$, respectively. Diamonds denote the results of fits to self-diffusion data. The dashed line is the prediction of the DMF model.

weakly interacting regime. In this section, we try to also interpret the viscosity data in this regime obtained from the numerical simulations within the chain model.

Figure 6 shows the shear viscosity obtained by NEBD simulations in planar Couette flow as a function of the magnetic field. The magnetic field was oriented either in flow or gradient direction. Different concentrations and dipolar interaction strengths are considered. Also shown are fits to the simulation results by the chain model, where the shape parameter B was used as a fitting parameter. The fits are found to describe the numerical data rather well. The shape parameters B obtained from those fits are shown in the right panel of figure 6. For weak dipolar interactions, the predictions of the DMF model $B \approx -\frac{2}{7}\chi_L$, the diffusion data (diamonds) and the viscosity data for the case where the magnetic field is oriented in the flow direction (open squares) are in fair agreement with each other. For stronger dipolar interactions, the viscosity data (filled squares) are also described by effective oblate particles, however with an even lower value of the shape parameter B. Therefore, B cannot be considered as a function of χ_L only, but depends on λ and ϕ separately. If the magnetic field is oriented in the gradient direction of the flow, however, the viscosity data (circles) are described by effective prolate ellipsoidal particles with $B > 0$ also depending on λ and ϕ separately.

Although these studies are only first steps towards a unified mean-field model valid for all interaction strengths, it appears that the chain model could indeed be a candidate for such a model. Of course, further investigations are necessary to verify or falsify this conjecture. In addition, determining the value of the shape parameter B seems not obvious, since it does not only depend on λ and ϕ but also on the orientation of the magnetic field with respect to the flow geometry. In the case of strong dipolar interactions, for which the model was developed originally [3], this difficulty seems less pronounced at least for weak flows. In order to obtain a better theoretical estimate of B in the weakly interacting regime, a careful study of the flow-induced structures would be very helpful. In particular, special attention should be paid to the differences between the structures if the magnetic field is oriented in flow and in gradient directions. Such studies could also answer the question whether the value of B obtained in the fits corresponds to real physical quantities or should rather be considered as an artefact of the description with an oversimplified model.

6. Conclusion and perspectives

We have performed equilibrium and non-equilibrium Brownian dynamics simulations of a ferrofluid model system with realistic interaction potentials. For sufficiently strong effective dipolar interaction strengths $\lambda^* \gtrsim 3$, the formation of chain-like structures in the presence of a magnetic field is observed. The cluster sizes are found to be exponentially distributed, in agreement with the predictions of the chain model. In the presence of a shear flow, the cluster size distribution is still of exponential form, but shifted towards smaller values. This flow-induced rupture of chains has already been anticipated for some time [5, 41, 53]. We also provide numerical evidence that this rupture of chains is responsible for pronounced shear thinning behaviour. The simulation results therefore support the main assumptions and results of the chain model for strongly interacting ferrofluids. More quantitative comparisons are neccessary in order to discuss the accuracy of the chain model predictions for rheological properties.

For weakly interacting ferrofluids, the DMF model is found to provide an accurate description of the magnetoviscous effect, supporting the results found in [24, 25]. Within the DMF model, weak dipolar interactions can be described approximately by effective oblate ferromagnetic particles. Since effective prolate, chain-like particles are present in the strongly interacting regime, we propose that the chain model can be extended to the moderate and weak interaction regime by allowing the shape factor of the effective particles to vary over the whole admissible range. By comparing the shape factor deduced from diffusion and rheological results with the estimate based on the DMF model, we observe fair agreement in the dilute, weakly interacting regime. If, however, the field is oriented in the gradient direction of the flow, the rheological data suggest effective prolate particles, contrary to the findings in the other cases. These results may serve as starting point for the development of a unified kinetic model applicable for all interaction strengths, for diffusion as well as rheological properties.

Acknowledgments

We are grateful for stimulating discussions with A O Ivanov, M Kröger, L M Pop, A Wiedenmann, and A Yu Zubarev. This work was supported by the German research foundation DFG SPP-1104 ‘Colloidal magnetic fluids’, grant no. HE 1108/8-1. PI was partially supported by the Alexander von Humboldt Foundation.

References

[1] Pop L M, Odenbach S, Wiedenmann A, Matoussevitch N and Bönnemann H 2005 Microstructure and rheology of ferrofluids *J. Magn. Magn. Mater.* **289** 303–6
[2] Odenbach S (ed) 2002 *Ferrofluids. Magnetically Controllable Fluids and Their Applications* (*Springer Lecture Notes in Phys.* vol 594) (Berlin: Springer)
[3] Zubarev A Yu and Iskakova L Yu 1995 Theory of physical properties of magnetic liquids with chain aggregates *JETP* **80** 857–66
[4] Zubarev A Yu and Iskakova L Yu 2000 Effect of chainlike aggregates on dynamical properties of magnetic liquids *Phys. Rev.* E **61** 5415–21
[5] Zubarev A Yu, Fleischer J and Odenbach S 2005 Towards a theory of dynamical properties of polydisperse magnetic fluids: effect of chain-like aggregates *Physica* A **358** 475–91
[6] Zubarev A Yu, Odenbach S and Fleischer J 2002 Rheological properties of dense ferrofluids. Effect of chain-like aggregates *J. Magn. Magn. Mater.* **252** 241–3
[7] Ivanov A O, Wang Z and Holm C 2004 Applying the chain formation model to magnetic properties of aggregated ferrofluids *Phys. Rev.* E **69** 031206

[8] Morozov K I and Shliomis M I 2004 Ferrofluids: flexibility of magnetic particle chains *J. Phys.: Condens. Matter* **16** 3807–18
[9] Mendelev V S and Ivanov A O 2004 Ferrofluid aggregation in chains under the influence of a magnetic field *Phys. Rev.* E **70** 051502
[10] Ivanov A O, Kantorovich S S, Mendelev V S and Pyanzina E S 2006 Ferrofluid aggregation in chains under the influence of a magnetic field *J. Magn. Magn. Mater.* **300** e206–9
[11] Larson R G 1999 *The Structure and Rheology of Complex Fluids* (New York: Oxford University Press)
[12] Huke B and Lücke M 2000 Magnetization of ferrofluids with dipolar interactions: a Born-Mayer expansion *Phys. Rev.* E **62** 6875–90
[13] Ivanov A O and Kuznetsova O B 2001 Magnetic properties of dense ferrofluids: an influence of interparticle correlations *Phys. Rev.* E **64** 041405
[14] Wang Z, Holm C and Müller H W 2002 Molecular dynamics study on the equilibrium magnetization properties and structure of ferrofluids *Phys. Rev.* E **66** 021405
[15] Ilg P and Hess S 2003 Nonequilibrium dynamics and magnetoviscosity of moderately concentrated magnetic liquids: a dynamic mean-field study *Z. Naturf.* a **58** 589–600
[16] Zubarev A Yu and Yushkov A V 1998 Dynamic properties of moderately concentrated magnetic liquids *JETP* **87** 484–93
[17] Satoh A, Chantrell R W, Coverdale G N and Kamiyama S 1998 Stokes dynamics simulations of ferromagnetic colloidal dispersions in a simple shear flow *J. Colloid Interface Sci.* **203** 233–48
[18] Satoh A, Chantrell R W and Coverdale G N 1999 Brownian dynamics simulations of ferromagnetic colloidal dispersions in a simple shear flow *J. Colloid Interface Sci.* **209** 44–59
[19] Morimoto H and Maekawa T 2001 Brownian dynamics analysis of cluster structures and magnetic characteristics of ferromagnetic particles subjected to a shear flow *Int. J. Mod. Phys.* B **15** 823–8
[20] Morimoto H, Maekawa T and Matsumo Y 2002 Nonequilibrium Brownian dynamics analysis of negative viscosity induced in a magnetic fluid subjected to both ac magnetic and shear flow fields *Phys. Rev.* E **65** 061508
[21] Ilg P and Kröger M 2005 Anisotropic self-diffusion in ferrofluids studied via Brownian dynamics simulations *Phys. Rev.* E **72** 031504
[22] Huang J P, Wang Z W and Holm C 2005 Computer simulations of the structure of colloidal ferrofluids *Phys. Rev.* E **71** 061203
[23] Wang Z and Holm C 2003 Structure and magnetic properties of polydisperse ferrofluids: a molecular dynamics study *Phys. Rev.* E **68** 041401
[24] Ilg P, Kröger M and Hess S 2005 Magnetoviscosity of semi-dilute ferrofluids and the role of dipolar interactions: comparison of molecular simulations and dynamical mean-field theory *Phys. Rev.* E **71** 031205
[25] Ilg P, Kröger M and Hess S 2005 Anisotropy of the magnetoviscous effect in ferrofluids *Phys. Rev.* E **71** 051201
[26] Kröger M, Ilg P and Hess S 2003 Magnetoviscous model fluids *J. Phys.: Condens. Matter* **15** S1403–23
[27] Rosensweig R E 1985 *Ferrohydrodynamics* (Cambridge: Cambridge University Press)
[28] Öttinger H C 1996 *Stochastic Processes in Polymeric Fluids* (Berlin: Springer)
[29] Barker J A and Henderson D 1976 Perturbation theory and equation of state for fluids. II. A successful theory of liquids *J. Chem. Phys.* **47** 4714
[30] Odenbach S 2002 *Magnetoviscous Effects in Ferrofluids* (*Springer Lecture Notes in Phys.*) (Berlin: Springer)
[31] Dhont J K G 1996 An introduction to dynamics of colloids *Studies in Interface Science* (Amsterdam: Elsevier)
[32] Coquelle E, Ilg P and Hess S 2006 Effect of hydrodynamic interactions and polydispersity on the dynamics of ferrofluids, in preparation
[33] Felderhof B U 2000 Magnetoviscosity and relaxation of ferrofluids *Phys. Rev.* E **62** 3848–54
[34] Evans D J and Morris G P 1990 *Statistical Mechanics of NonEquilibrium Liquids* (New York: Academic)
[35] Ilg P and Kröger M 2002 Magnetization dynamics, rheology, and an effective description of ferromagnetic units in dilute suspension *Phys. Rev.* E **66** 021501
Ilg P and Kröger M 2003 *Phys. Rev.* E **67** 049901 (erratum)
[36] Hess S 2000 Flow properties and structure of anisotropic fluids studied by non-equilibrium molecular dynamics, and flow properties of other complex fluids: polymeric liquids, ferro-fluids and magneto-rheological fluids *Advances in the Computer Simulation of Liquid-Crystals* ed P Parisi and C Zannoni (Dordrecht: Kluwer) pp 189–233
[37] Holm C and Weis J J 2005 The structure of ferrofluids: a status report *Curr. Opin. Colloid Interface Sci.* **10** 133–40
[38] Teixeira P I C, Tavares J M and Telo da Gama M M 2000 The effect of dipolar forces on the structure and thermodynamics of classical fluids *J. Phys.: Condens. Matter* **12** R411–34

[39] Tlusty T and Safran S A 2000 Defect-induced phase separation in dipolar fluids *Science* **290** 1328–31
[40] Huke B and Lücke M 2001 Equilibrium magnetization of dipolar interacting ferrofluids *Magnetohydrodynamics* **37** 243–53
[41] Hess S, Weider T and Kröger M 2001 Viscous properties and structure of ferro-fluids and magneto-rheological fluids. Non-equilibrium molecular dynamics (NEMD) studies of simple model systems *Magnetohydrodynamics* **37** 297–306
[42] Hess S, Schwarzl J F and Baalss D 1990 Anisotropy of the viscosity of nematic liquid crystals and of oriented ferro-fluids via nonequilibrium molecular dynamics *J. Phys.: Condens. Matter* **2** 279
[43] Butter K, Bomans P H, Frederik P M, Vroege G J and Philipse A P 2003 Direct observation of dipolar chains in iron ferrofluids by cryogenic electron microscopy *Nat. Mater.* **2** 88–91
[44] Klokkenburg M, Dullens R P A, Kegel W K, Erné B H and Philipse A P 2006 Quantitative real-space analysis of self-assembled structures of magnetic dipolar colloids *Phys. Rev. Lett.* **96** 037203
[45] Hoell A, Wiedenmann A, Heyen U and Schüler D 2005 *Physica* B **350** e309–14
[46] Iskakova L Yu and Zubarev A Yu 2002 Effect of interaction between chains on their size distribution: strong magnetic field *Phys. Rev.* E **66** 041405
[47] Cates M E and Candau S J 1990 *Condens. Matter* **2** 6869
[48] Martsenyuk M A, Raikher Yu L and Shliomis M I 1974 On the kinetics of magnetization of suspension of ferromagnetic particles *Sov. Phys.—JETP* **38** 413–6
[49] Levi A C, Hobson R F and McCourt F R 1973 Magnetoviscosity of colloidal suspensions *Can. J. Phys.* **51** 180
[50] Brenner H and Weissman M H 1972 Rheology of a dilute suspension of dipolar spherical particles in an external field: II Effect of rotary Brownian motion *J. Colloid Interface Sci.* **41** 499–531
[51] Blums E, Cebers A and Maiorov M M 1997 *Magnetic Fluids* (Berlin: de Gruyter)
[52] Pshenichnikov A F, Mekhonoshin V V and Lebedev A 1996 Magneto-granulometric analysis of concentrated ferrocolloids *J. Magn. Magn. Mater.* **161** 94–102
[53] Odenbach S and Störk H 1998 Shear dependence of field induced contributions to the viscosity of magnetic fluids at low shear rates *J. Magn. Magn. Mater.* **183** 188–94
[54] Lal J, Abernathy D, Auvray L, Diat O and Grübel G 2001 Dynamics and correlations in magnetic colloidal systems studied by x-ray photon correlation spectroscopy *Eur. Phys. J.* E **4** 263–71
[55] Bacri J-C, Cebers A, Bourdon A, Demouchy G, Heegaard B M and Perzynski R 1995 Forced Rayleigh experiment in a magnetic fluid *Phys. Rev. Lett.* **74** 5032–5
[56] Bacri J-C, Cebers A, Bourdon A, Demouchy G, Heegaard B M, Kashevsky B and Perzynski R 1995 Transient grating in a ferrofluid under magnetic field: effect of magnetic interactions on the diffusion coefficient of translation *Phys. Rev.* E **52** 3936–42
[57] Kollmann M, Hund R, Rinn B, Nägele G, Zahn K, König H, Maret G, Klein R and Dhont J K G 2002 Structure and tracer-diffusion in quasi two-dimensional and strongly asymmetric magnetic colloidal mixtures *Europhys. Lett.* **58** 919–25
[58] Morozov K I 1993 The translational and rotational diffusion of colloidal ferroparticles *J. Magn. Magn. Mater.* **122** 98–101
[59] Blums E 1995 Some new problems of complex thermomagnetic and diffusion-driven convection in magnetic colloids *J. Magn. Magn. Mater.* **149** 111–5
[60] Hernández-Contreras M, González-Mozuelos P, Alarcón-Waess O and Ruíz-Estrada H 1998 Long-time self-diffusion in a model ferrofluid *Phys. Rev.* E **57** 1817–23
[61] Hernández-Contreras M and Ruíz-Estrada H 2003 Transport properties of ferrofluids *Phys. Rev.* E **68** 031202
[62] Ilg P 2005 Anisotropic diffusion in nematic liquid-crystals and in ferrofluids *Phys. Rev.* E **71** 051407
[63] Prager S 1955 Interaction of rotational and translational diffusion *J. Chem. Phys.* **23** 2404–7
[64] Hess S and Müller R 1974 On the depolarized Rayleigh scattering from macromolecular and colloidal solutions-anisotropy of the diffusional broadening *Opt. Commun.* **2** 172–4